AIP Applied Physics Letters

Fabrication of bioinspired omnidirectional and gapless microlens array for wide field-of-view detections

Hewei Liu, Feng Chen, Qing Yang, Pubo Qu, Shengguan He, Xianhua Wang, Jinhai Si, and Xun Hou

Citation: Applied Physics Letters **100**, 133701 (2012); doi: 10.1063/1.3696019
View online: http://dx.doi.org/10.1063/1.3696019
View Table of Contents: http://scitation.aip.org/content/aip/journal/apl/100/13?ver=pdfcov
Published by the AIP Publishing

Fabrication of bioinspired omnidirectional and gapless microlens array for wide field-of-view detections

Hewei Liu,[1] Feng Chen,[1,a)] Qing Yang,[2] Pubo Qu,[1] Shengguan He,[1] Xianhua Wang,[1] Jinhai Si,[1] and Xun Hou[1]
[1]*Key Laboratory for Physical Electronics and Devices of the Ministry of Education and Key Laboratory of Photonics Technology for Information of Shaanxi Province, School of Electronics and Information Engineering, Xi'an Jiaotong University, Xi'an 710049, People's Republic of China*
[2]*State Key Laboratory for Manufacturing System Engineering, Xi'an Jiaotong University, Xi'an 710049, People's Republic of China*

(Received 15 November 2011; accepted 5 January 2012; published online 26 March 2012)

Microlens arrays on curvilinear surfaces are highly desirable for wide field-of-view imaging and sensing systems. However, it is technically challenging to fabricate these structures. This letter reports a simple method to machine close-packed microlenses on curvilinear surfaces as inspired by the insect eyes, which involves a femtosecond-laser-based microfabrication and a thermomechanical bending process. Over 7600 hexagonal-shaped microlenses with a diameter of 50 μm were fabricated on a hemispherical poly (methyl methacrylate) shell, which is similar to the compound eyes of insects. The optical performances of the microlens array were demonstrated by the abilities of high-resolution imaging and large view-angle focusing. © *2012 American Institute of Physics*. [http://dx.doi.org/10.1063/1.3696019]

Omnidirectionally arranged optical elements allow for the wide field-of-view (FOV) imaging and the high-sensitivity detection[1–3] and have reduced components and minimized volume compared to the traditional planer devices. For example, compound eyes in nature,[4,5] which are commonly composed of 10-30 000 (depends on the species of the insects) spherical-distributed and hexagonal-shaped ommatidia with diameters ranging from 10 μm to 100 μm, are sensitive to moving objects with the angle of FOV close to 180°. This wide FOV enables insects to escape from dangers. Therefore, artificial compound eyes with such features have attracted a great deal of research interest. However, fabrication of optical units onto curvilinear surfaces is still challenging because most current fabrication processes are planer in nature. In recent years, several strategies have been developed for non-planer microfabrications.[6–10] Although these techniques demonstrate the ability to produce microstructures on the curvilinear surfaces, they are high-cost, complex, and require long processing time. There is still an unmet need for a simple and cost-effective method.

In this letter, we introduce a simple yet practical route to fabricate close-packed microlenses onto curvilinear surfaces for wide FOV. The fabrication process involves a femtosecond (fs)-laser-based process to create close-packed microlenses on flat plastic films, followed by a thermomechanical bending process to that geometrically transformed planer microlens arrays to the curvilinear shapes. In the example, we presented here, thousands of hexagonal-shaped microlenses were produced on a poly (methyl methacrylate) (PMMA) hemispherical shell, which is demonstrated in Fig. 1(a). The diameter of the shell is about 3.5 mm, and the height of dome is about 1.6 mm. The investigation of the microlenses on the dome with a scanning electronic microscope (SEM), as shown in Fig. 1(b), indicates a compound-eye-like structure with uniform and hexagonal-shaped microlenses.

The fabrication process was started with the manufacturing of planer microlens arrays on the PMMA films by the fs-laser microfabrication and replication process, Fig. 2(a) (steps 1 to 4). We used the previously developed methodology to fabricate concave microlenses on a silica glass chip ($30 \times 30 \times 2$ mm^3), which offers a scalable shape-controllable approach to generate large-area concave microlens arrays on glasses.[11] The sample surface was exposed to the femtosecond laser pulses (wavelength: 800 nm; pulse duration: 30 fs; and repetition rate: 1 kHz) spot-by-spot by focusing the laser beam via an objective lens (Nikon, N.A. = 0.5), resulting in the modification of materials in the focal spot. The exposure time, t, which was controlled by a fast mechanical shutter, was set at 500 ms in the experiment,[12] and the laser power was set at 2.5 mW. By translating the sample using a 3D-stage, an array of exposure spots was created, as shown in Fig. 2(b). They are hexagonal arranged with an interspacing of 50 μm. After a 45-min chemical treatment (at room temperature) using a 5% hydrofluoric acid solution (diluted by ionized water), concave microlens array were achieved on the sample surface. The SEM image of the microstructure demonstrates its uniformity and smooth surface, Fig. 2(d).

Serving the silica glass with concave microlenses as a molding template, the convex microlens array was replicated on the planar PMMA film. We employed PMMA as a material to fabricate microlens arrays because of its excellent transparency for visible light and the ability of irreversible deformation during the thermomechanical bending process. Liquid mixture of PMMA and chloroform with a weight ratio of 1:10 was spun onto the molding template (500 rpm for 30 s) and cured at room temperature for 4 h. The thickness of the demolded film was about 130 μm.

a)Author to whom correspondence should be addressed. Electronic mail: chenfeng@mail.xjtu.edu.cn. Tel.: 86 029 82665105. Fax: 86 029 82665105.

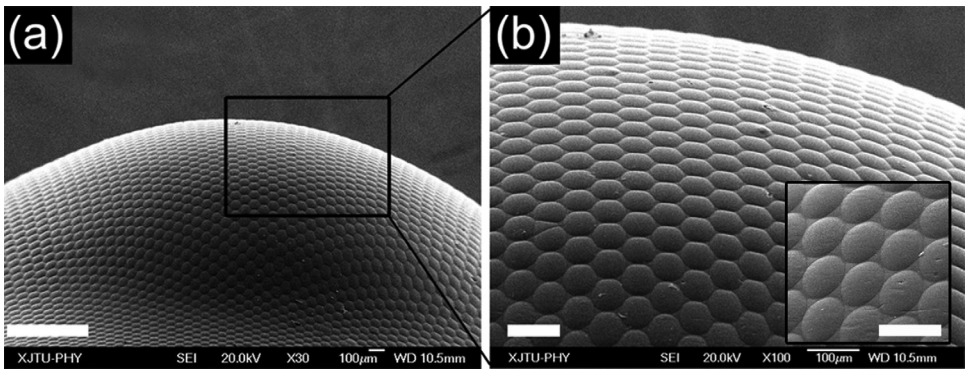

FIG. 1. (a) The morphology of the omnidirectional microlens array observed via an SEM. The scale bar is 1 mm. (b) SEM observation of the microlenses on the top of hemispherical shell. The scale bar is 100 μm. Inset: the microlenses on the outer ring of the dome (the scale bar is 100 μm).

Subsequently, we bended the planer PMMA film with the microlens array to the hemispherical shell using the thermomechanical bending process. A hemispherical lens with the diameter of 3.5 mm was heated to 95 °C and pushed into the PMMA film slowly from the surface without the microlens array (Fig. 2(a), steps 5 and 6, respectively). The microlens film was consequently wrapped onto the glass dome. After a few minutes when it dropped to room temperature, the hemispherical shell was torn off with the microlens array (steps 7 and 8). In the bending process, the heating temperature, which depends to the thickness of the microlens films, should be closed to the glass transition temperature of PMMA (~104 °C), ensuring the rubbery transition of the PMMA film. For lower temperatures (<80 °C) or thick films (>200 μm), the rubbery transition of PMMA was not occurred, making it difficult to wrap the film tightly onto the hemispherical lens. However, high temperatures (>120 °C) with thin films (<100 μm) will enhance the fluid property of the PMMA, resulting in the damages of the microlenses. Therefore, for the thickness of 120 μm, the temperature of 95 °C is the optimized value to bend the planer film to the spherical shell with the intact microlens array on it. Despite of this, the unequal distribution of strains on the hemisphere was still resulted from the thermomechanical bending process. The inserted SEM image in Fig. 1(b) shows the microlenses on the outer ring of the dome, in which narrow gaps can be observed. During the bending process that converted the planer sheet to the 3D structure, close-packed microlenses were stretched and separated with each other, leading to the results shown in the insertion of Fig. 1(b). On the top of dome, however, the stains are relatively small, enabling the retention of gapless microlens array as shown in Fig. 1(b).

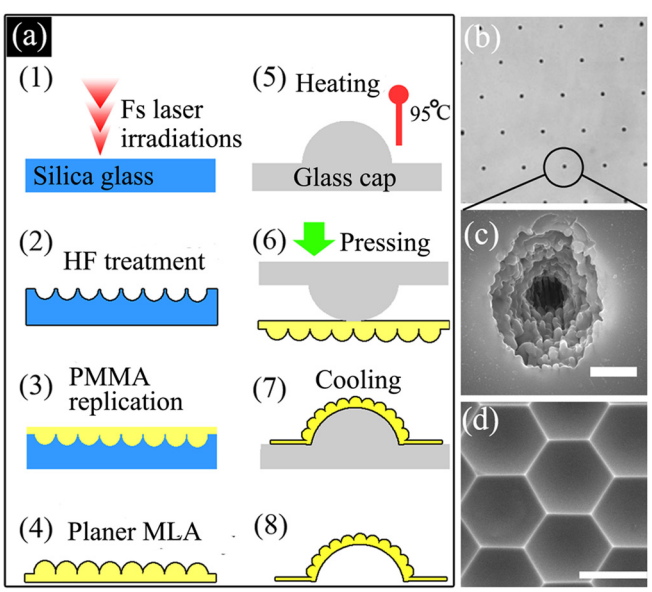

FIG. 2. (Color online) (a) The schematic diagrams of the fabrication process. Steps 1 and 2 depict the fabrication of molding template of concave microlens array using the femtosecond laser irradiations followed by HF acid etching process. Steps 3 and 4 show the replication of convex microlens array on the PMMA film. Steps 5 to 8 show the thermal extrusion process, which transformed the planer PMMA film with microlens array to the hemispherical shape. (b) The laser exposure spots which are captured by an optical microscope. (c) SEM observation of an exposure spot. The scale bar is 2 μm. (d) SEM observation of the morphology of the molding template. The scale bar is 50 μm.

We measured the 3D and 2D profiles of the microlenses on the top of the shell using a laser confocal microscope (OPTELICS, S130), as shown in Figs. 3(a) and 3(b), respectively. Consequently, the diameter and height of a microlens are 50 μm and 7.2 μm, respectively. For a compound eye of insects, each ommatidium can produce individual images of the projected object; therefore the resolution of the image is determined by the number of ommatidia. Here, we estimated the total number of the microlenses distributed on the hemispherical shell with the total area of the dome divided by an area of a microlens and obtained a result of ~7600. Besides, the angle between two neighboring ommatidia is about 2°. These results are very close to the compound eyes in nature.[2] The focal length of the microlenses could be calculated according to $f = (R^2 + h^2)/2h(n-1) - h(n-1)$, where R and h are the radius and height of microlenses, respectively, and n is the reflective index of PMMA. Given $n = 1.49$, $R = 25$ μm, and $h = 7.2$ μm, we get $f = 92.4$ μm.

To demonstrate the ability of the large FOV detection of the fabricated omnidirectional microlens array, we used a 632-nm He-Ne laser beam with an aperture of 1 mm to irradiate the hemispherical shell with different incident angles, θ, and captured their focal spots generated through the microlenses on the dome by an objective lens (Nikon, N.A. = 0.15) and a CCD camera. The setup is schematically shown in Fig. 3(c). For $\theta = 0°$, 70°, and −70°, the microscope images of the focal spots are shown in Fig. 3(d). Note that slight distortions of the focal spots are observed at $\theta = \pm 70°$ (see insertions in Fig. 3(d)), indicating the impact of thermomechanically bending process on the focusing capability of the microlens array. According to the diameter

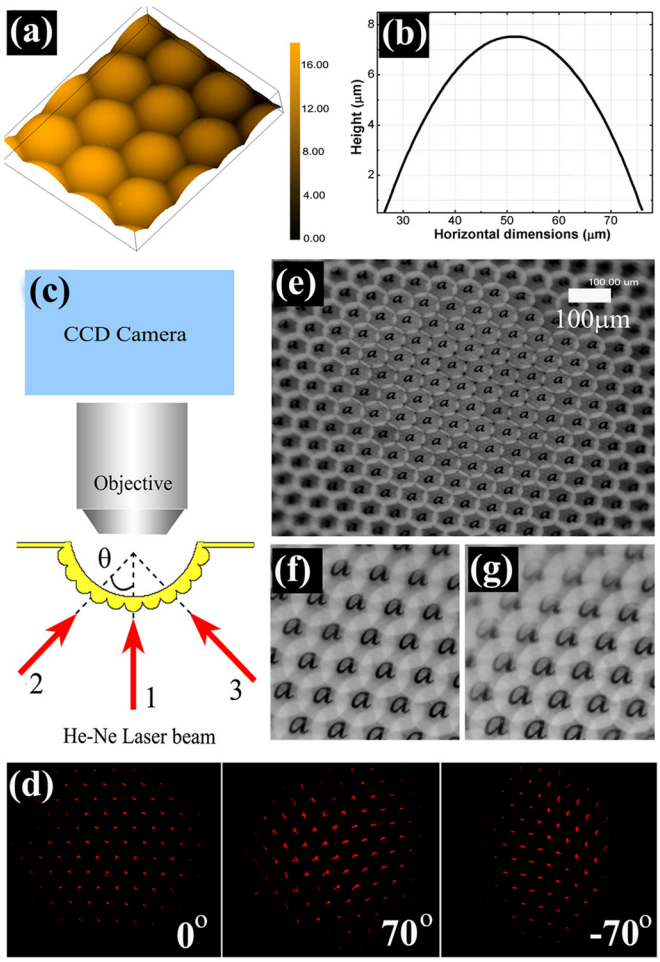

FIG. 3. (Color online) (a) 3D profiles of the microlenses on the top of the hemispherical shell. The result was obtained by a laser confocal microscope. (b) Cross-sectional profile of a microlens shown in (a). (c) Optical setup of system which demonstrates the large view-angle focusing property of the microlens array. (d) The focal spots captured by the CCD camera when the incoming laser angel is 0°, 70°, and −70°. (e) Imaging performance of the microlens array. The result was obtained via a 5× objective lens. (f) and (g) Imaging performance of the microlenses on the top and side of hemispherical shell, respectively. The result was obtained via a 20× objective lens.

and height of the shell, the calculated FOV of the microlens array is about 162°. Here, we should argue that parts of focal spots were blocked by the shell when $\theta > \pm 70°$, and we failed to capture them in the CCD camera. Despite this, the FOV of 140° is still much wider than the planer compound-eye systems,[13–15] which are commonly less than 90°. More importantly, we did not observe obvious distortions of focal spots from the microscope images. It is helpful to improve imaging performance of the microlens array, which was demonstrated by an imaging test using a microscope system equipped with a tungsten light source and a CCD camera. By setting a transparent film with a typed alphabet, "a," between the light source and the microlens array, real images were created and captured by the CCD camera. Figure 3(e) shows the images which were observed by a 5× objective lens. The images created via the microlenses on the top and side of dome, which were captured by a 20× objective lens, are shown in Figs. 3(f) and 3(g), respectively. Clear images of alphabet, "a," were observed in figures, demonstrating the perfect imaging properties of the fabricated microlens array.

The ability of wide FOV detection of the natural compound eyes arises from not only the omnidirectionally arranged ommatidia but also the independent imaging ability of each ommatidium which can collect incident light through a narrow range of angular acceptance and independently contributes to the wide FOV detection. In our study, only the exterior of microlenses was fabricated, resulting in the multiple images by simple projection optics. But independent imaging was not the focus of this work. Additionally, because the microlenses were fabricated on a hollow and rigid hemispherical dome, it would provide several potential applications by integrating with other devices. For example, it could be used as a light-emitting diode shaper, which would helpful to eliminate the non-uniformity of the light distribution of the point light source and improve the light transparency.[16–18]

In conclusion, we have demonstrated a simple method to fabricate microlenses on curvilinear surfaces by the femtosecond laser microfabrication and the thermomechanical bending process. Over 7600 hexagonal-shaped microlenses were fabricated on a PMMA hemispherical shell. The theoretical value of FOV of the microlens array reaches to 162° and its ability of large view-angle focusing was also demonstrated experimentally. Our approach offers several advantages, such as low-cost, easy manipulation, and reproducible fabrication process. Additionally, the method can be used to fabricate other microstructured curvilinear surfaces.

This work is support by National Science Foundation of China under the Grant No. 61176113 and the Fundamental Research Funds for the Central Universities

[1]D. Zhu, C. Li, X. Zeng, and H. Jiang, Appl. Phys. Lett. **96**, 081111 (2010).
[2]K.-H. Jeong, J. Kim, and L. P. Lee, Science **312**, 557 (2006).
[3]H. C. Ko, M. P. Stoykovich, J. Song, V. Malyarchuk, W. M. Choi, C.-J. Yu, J. B. Geddes, J. Xiao, S. Wang, Y. Huang *et al.*, Nature **454**, 748 (2008).
[4]M. F. Land, Annu. Rev. Entomol. **42**, 147 (1997).
[5]J. W. Duparré and F. C. Wippermann, Bioinspir. Biomim. **1**, R1 (2006).
[6]E. P. Chan and A. J. Crosby, Adv. Mater. **18**, 3238 (2006).
[7]C. Li, A. Ji, and Z. Cao, Appl. Phys. Lett. **90**, 164102 (2007).
[8]W. R. Childs and R. G. Nuzzo, Adv. Mater. **16**, 1323 (2004).
[9]A. M. Bowen and R. G. Nuzzo, Adv. Funct. Mater. **19**, 3243 (2009).
[10]R. Mukherjee, A. Sharma, G. Patil, D. Faruqui, and P. S. G. Pattader, Bull. Mater. Sci. **31**, 249 (2008).
[11]F. Chen, H. Liu, Q. Yang, X. Wang, C. Hou, H. Bian, W. Liang, J. Si, and X. Hou, Opt. Express **18**, 20334 (2010).
[12]A long exposure time will help to fabricate uniform concave structures, but sacrifice the processing efficiency. And the used value of 500 ms is an optimized result in the previous experiment shown in Ref. 11.
[13]A. Brückner, J. Duparré, A. Bräuer, and A. Tünnermann, Opt. Express **14**, 12076 (2006).
[14]J. Duparré, P. Schreiber, A. Matthes, E. P. Severin, A. Bräuer, A. Tünnermann, R. Völkel, M. Eisner, and T. Scharf, Opt. Express **13**, 889 (2005).
[15]K. Hamanaka and H. Koshi, Opt. Rev. **3**, 264 (1996).
[16]C. J. Yang, S. H. Liu, H. H. Hsieh, C. C. Liu, T. Y. Cho, and C. C. Wu, Appl. Phys. Lett. **91**, 253508 (2007).
[17]T. R. M. Sales, Proc. SPIE **5175**, 109 (2003).
[18]S. Chang, J. Yoon, H. Kim, J. Kim, B. Lee, and D. H. Shin, Opt. Lett. **31**, 3016 (2006).